Research Article

Hasan Shakir Majdi, Mahmoud A. Mashkour, Laith Jaafer Habeeb*, and Marko Ilic

Mixed convection around a circular cylinder in a buoyancy-assisting flow

https://doi.org/10.1515/cls-2022-0008
Received Oct 05, 2021; accepted Nov 29, 2021

Abstract: In this paper, the effect of mixed convection on the flow behavior and heat transfer around a circular cylinder disclosed to a vertically upward laminar air stream is numerically examine. The buoyancy-aided flow is utilized to eliminate and control the vortex shedding of the cylinder. The influence of the Grashof number, $0 \leq Gr \leq 6000$, the flow and thermal patterns, as well as the local and mean Nusselt number, is investigated at a constant Reynolds number of 100. The unsteady Navier-Stokes's equations are solved employing a finite-volume method to simulate numerically the velocity and temperature fields in time and space. The results showed periodic instability in the flow and thermal fields for a range of Grashof number $Gr \leq 1300$. Also, there is critical value of Grashof number for stopping this instability and the vortex shedding formed behind the cylinder, by the effect of heating. Thus, by increasing Grashof number between $1400 \leq Gr \leq 4000$, the periodic flow vanishes and converts into steady flow with twin eddies attached to the cylinder from the back. Furthermore, as Grashof number increases behind $Gr \geq 5000$, the flow becomes completely attached to the cylinder surface without any separation.

Keywords: Mixed convection, circular cylinder, vortex shedding, adding flows

1 Introduction

Vortex shedding behind cylinders is an interesting topic for many researchers. This is due to that forming vortex shedding behind these bodies causes unfavorable oscillations in the aero- or hydro-dynamic loads, leading to undesirable vibrations in the bodies' structures. Therefore, a huge effort has been assigned in an attempt to reduce or eliminate the effect of vortex shedding. The literature shows that there are various methods to eliminate or control the vortex shedding like suction, blowing, rotating the body, surface roughness, and heating the cylinder, see for example [1–5].

Indeed, this phenomenon in mixed convective flow can lead to very intricate physical circumstances due to the high interaction amongst the buoyancy effects of free convection, effects of forced flow, and the effects of secondary flows generated behind the solid bodies. Many works have discussed this problem. Badr [6] investigated the mixed convective flow and heat transfer about a horizontal cylinder for contra and parallel flows for Reynolds numbers less than 40. Chang and Sa [7] also investigated the flow behavior, Nusselt number variations, and drag coefficient from a cylinder at Reynolds numbers of 100 and Grashof number between104 for cooling and 104 for heating. It was found that the vortex shedding can be stopped by increasing Grashof number higher than 1500. In addition, Wang [8] studied mixed convection from an isothermal needle containing a hot tip for contra and assisting flows. Michaux and B'elorgey [9] performed some experiments to study the effect of buoyancy forces of mixed convection on the wake flow behavior behind a circular cylinder the Reynolds numbers of greater than 130. They observed that the forced convection is predominant when Richardson number is higher than 0.5, while the natural convection becomes the dominant for Richardson number less than 0.5. Varaprasad *et al.* [10] examined the effect of buoyancy forces on the mixed convective flow over a circular cylinder and tested its impact on Nusselt number distributions, drag coefficient, wake structure, and Strouhal number. They reported that the increase in Grashof number could also increase the drag coefficient around the cylinder.

Moreover, Kieft *et al.* [11] investigated the flow wake structure backward a heated cylinder located in a horizontal crossflow at constant Reynolds number of 75 and Richardson number ranging between 0 and 1. They found that the heating of cylinder produces vortex shedding in the

***Corresponding Author: Laith Jaafer Habeeb:** Training and Workshop Center, University of Technology, Baghdad, Iraq; Email: Laith.J.Habeeb@uotechnology.edu.iq
Hasan Shakir Majdi: Department of Chemical Engineering and Petroleum Industries, Al-Mustaqbal University College, Hillah, Babil, Iraq
Mahmoud A. Mashkour: Mechanical Engineering Department, University of Technology, Baghdad, Iraq
Marko Ilic: Faculty of Mechanical Engineering, University of Nis, Nis, Serbia

rear of cylinder with lower and upper vortices have diverse strengths. Biswas and Sarkar [12] studied similar case of Kieft *et al.* [11] but for range of Reynolds numbers of 10-45. Interestingly, the results revealed that heat the cylinder and producing buoyancy forces trigger the vortex shedding to be occurred at low Reynolds number. For example, it was found that at Richardson number of 1.4, the vortex shedding takes place at low Reynolds number of 10, and by increasing Richardson number to value of 2, the vortex shedding happens at Reynolds number of 45. Sharma *et al.* [13] studied mixed convective flow across a square cylinder for Richardson 0-1 and Reynolds number 1-40. Their investigation did not notice any generation for a vortex shedding behind the cylinder for these ranges of Richardson and Reynolds numbers; however, a consistently steady flow was shown without any shedding. Gandikota *et al.* [14] examined mixed convective flow around a circular cylinder placed inside a vertical plate channel for two cooling and heating cases at Richardson's numbers of −0.5 and 0.5, respectively, for a Reynolds number ranging between 50 and 150. Their results indicated using a channel with a higher blockage ratio creates a considerable delay in the separation phenomena of the hydrodynamic boundary layer on the cylinder surface. Guill'en *et al.* [15] performed an experimental investigation about unsteady mixed convective flow over an isothermal cylinder in a contra-flow situation inside a vertical plate duct at Reynolds number of 170. They realized the influence of duct wall on the formation of flow wake in the back of cylinder. Moreover, Sanyal and Dhiman [16] tested the interactions amongst the wakes formed behind two square cylinders under the effect of mixed convection for Richardson number between and Reynolds number between 1-40, and for heavy liquid that possesses Prandtl number of 50. Chatterjee and Mondal [17–22] have made many studies about the effects of buoyancy forces on heat transfer and flow behavior about a cylinder.

The current literature highlighted that the increase in Grashof number might provoke an elimination for the vortex shedding; however, the influences of the buoyancy forces on eliminating the vortex shedding behind a cylinder in an assisting flow has been investigated yet. Therefore, the current study aims to test the buoyancy effects of mixed convection from a circular isothermal cylinder positioned in an upward vertical stream on the flow behavior and heat transfer characteristics. In this paper, we present the physical problem and the equations that govern the flow and thermal fields. Then, the numerical method that was used to solve the governing equations is briefly described. After that, the results and their discussion are outlined. Lastly, we draw the study's findings in the conclusion section.

2 Physical problem and governing equations

Figure 1 shows the schematic diagram for the geometry of the considered problem in conjunction with the system coordinates. Briefly, the problem composes of an unbounded circular cylinder of diameter D heated isothermally at a fixed temperature T_h and subjected to an upward vertical air stream of velocity v_o and temperature T_o. The gravity acts downward, while the buoyancy forces generated due to heating the cylinder act upward.

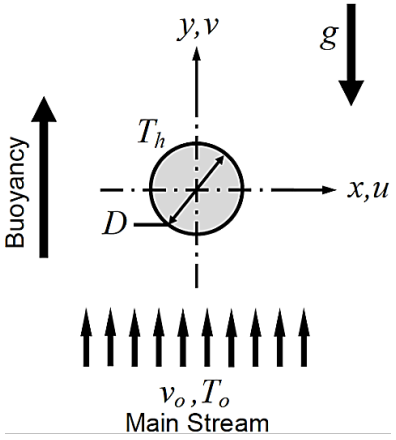

Figure 1: The physical problem under consideration

The standard mass, momentum, and energy equations described below in the non-dimensional form, are used to calculate the flow and temperature fields around the cylinder, and then the amount of heat released from the cylinder, for a transient, laminar, incompressible, two-dimensional mixed convective flow as follows:

$$\frac{\partial u}{\partial x} + \frac{\partial v}{\partial y} = 0, \tag{1}$$

$$\frac{\partial u}{\partial t} + \left(u\frac{\partial u}{\partial x} + v\frac{\partial u}{\partial y}\right) = \frac{1}{Re}\left(\nabla^2 u\right) - \frac{\partial p}{\partial x}, \tag{2}$$

$$\frac{\partial v}{\partial t} + \left(u\frac{\partial v}{\partial x} + v\frac{\partial v}{\partial y}\right) = \frac{1}{Re}\left(\nabla^2 v\right) - \frac{\partial p}{\partial y} + RiT, \tag{3}$$

$$\frac{\partial T}{\partial t} + \left(u\frac{\partial T}{\partial x} + v\frac{\partial T}{\partial y}\right) = \frac{1}{Re \cdot Pr}\left(\nabla^2 T\right), \tag{4}$$

where u and v are the non-dimensional velocities in horizontal and vertical orientations, respectively; T, p and t are the non-dimensional temperature, pressure, and time,

respectively. We used the following dimensional parameters for obtaining the aforementioned non-dimensional equations:

$$u = \frac{u'}{v_o}, \quad v = \frac{v'}{v_o}, \quad x = \frac{x'}{D}, \quad y = \frac{y'}{D}, \quad p = \frac{p'}{\rho v_o^2},$$
$$t = \frac{t'}{v_o D}, \quad T = \frac{T' - T_o}{T_h - T_o}$$

The principal dimensionless groups that control this kind of flow are Reynolds number Re, Richardson number Ri, and Prandtl Pr, which are defined as follows:

$$Re = \frac{v_o \rho D}{\mu}, \quad Ri = \frac{Gr}{Re^2}, \quad Pr = \frac{c_p \mu}{k}, \tag{5}$$

where, c_p, μ and ρ are the fluid heat capacity, the fluid dynamic viscosity, and the fluid density. Gr is the Grashof number as follows:

$$Gr = \frac{\rho^2 \cdot g \cdot \beta D^3 (T_h - T_o)}{\mu^2}, \tag{6}$$

where, k is the fluid thermal conductivity, and g the acceleration due to the earth gravity.

Local Nusselt number Nu_l represents the local heat transfer from the hot surface around the cylinder, and is calculated as:

$$Nu_l = \frac{hD}{k} = -\frac{\partial T}{\partial n}, \tag{7}$$

where, h is the local convective heat transfer coefficient around the cylinder perimeter, and n is the direction perpendicular to the cylinder wall. Then, this quantity is integrated over the cylinder surface to determine mean heat transfer Nu.

3 Numerical method

The aforementioned governing Eqs. (1)–(4) along with the boundary conditions elaborated in Eq. (8) below, are solved numerically employing a finite-volume method based on the SIMPLEC algorithm described in (Doormal and Raithby [23]). In this method, the temporal discretization is conducted by a second order implicit Adams- Bashforth scheme. Whereas, a second order upwind scheme is used for discretizing the convective terms, and a central difference scheme is used for discretizing the diffusive terms, in both the momentum and energy equations. The Courant-Friedrichs-Lewy and the grid Fourier number criteria are employed to avoid any computational oscillations. For convergence, the time interval was taken to be changed between 0.001 and 0.01 to calculate an optimal value for less numerical time, but with satisfactorily precise results. An interpolation method based on a body-force-weighted pressure technique is utilized for interpolating the interface pressure from the cell center value. The discretized equations are then numerically solved by an in-house solver. In the current computations, we used non-uniform computational mesh with fine clustering distributions in the vicinity of the cylinder surface walls for accurate calculation for the bigger variables' gradients. Figure 2 displays the computational mesh used for the whole computational domain.

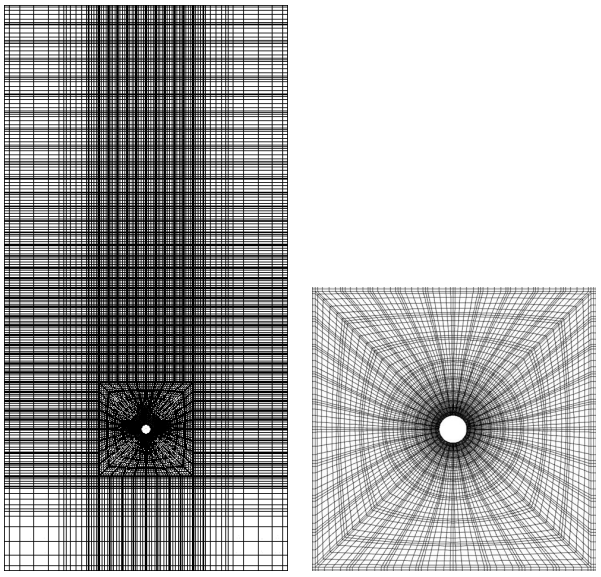

Figure 2: (Left) The computational grid for the entire domain, (Right) Zooming for the mesh around the cylinder

The boundary conditions that are employed in the present study can be expressed as:

$$\begin{aligned}
&u_o = 0, \quad v_o = 1, \quad T_o = 0, && \text{at Inlet} \\
&\frac{\partial u}{\partial y} = 0, \quad \frac{\partial v}{\partial y} = 0, \quad \frac{\partial T}{\partial y} = 0, && \text{at Outlet} \\
&\frac{\partial u}{\partial x} = 0, \quad \frac{\partial v}{\partial x} = 0, \quad \frac{\partial T}{\partial x} = 0, && \text{at Artificial} \\
& && \text{vertical borders} \\
&u = v = 0, \quad T_h = 1, && \text{at cylinder wall} \\
& && (0 < \theta^\circ < 360).
\end{aligned} \tag{8}$$

A mesh sensitivity study is performed to choose the best economic grid size. The numerical solution was checked for a mesh independency using different non-uniform mesh sizes S1, S2, S3, S4, S5, and S6, as shown in Table 1. This study was performed for different pertinent parameters. It was found that the mesh size S3 of (120×298) along x and y directions, respectively, can be used with an error less than 0.1%.

Table 1: Mesh sizes employed to examine the mesh independency

Mesh	($\Delta x \times \Delta y$)
S1	(92 × 235)
S2	(102 × 255)
S3	(120 × 298)
S4	(136 × 340)
S5	(150 × 375)

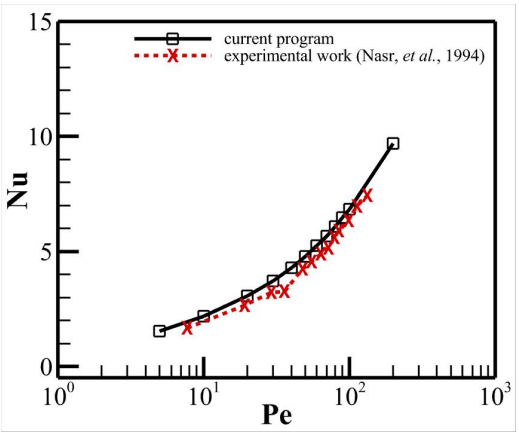

Figure 3: Verification for the numerical algorithm employed in our code

The accuracy of our numerical program was verified by comparing its results with experimental results previously published Nasr *et al.* [24] for the problem of forced convection about a cylinder of 12.7 mm diameter, and embedded in porous medium, which compromises from aluminum spheres of 12.23 mm diameter. Fixed porosity medium of 0.37 with thermal conductivity ratio of 8.7 were used. This comparison is demonstrated in Figure 3, and depicts a good matching between the experimental results and the numerical results of our code.

4 Results and discussion

In the present study, the numerical results were obtained for Prandtl number $Pr = 0.71$ for air as working fluid, and at constant Reynolds number of Re = 100. Figures 4–9 show the vorticity, streamlines, and isotherms patterns around the heated cylinder for different Grashof numbers $Gr = 0$–6000. It is shown in Figure 4 that at $Gr = 0$ and 1300 the mixed convective flow over the cylinder body generates a periodic secondary flow, which is called Van Karman vortex street. Also, as Grashof number increases, the van Karman vortex street at the cylinder back vanishes, and the flow converts completely to a steady flow with double eddies called wake attached to the cylinder back, as shown in Figure 6. The breakdown of the Van Karman vortex street happens probably by the reason of that the points of the flow separation on the right and left sides of the cylinder wall move downstream by the impact of the buoyancy forces as Grashof number increases. Moving of the separation locations downstream the cylinder wall might raise from the interactions between the eddies; consequently, vanishing of the Van Karman vortex street takes place and the flow turns completely into symmetric steady flow with stationary twin vortices behind the cylinder. It can also see that these twin eddies shrink considerably as Grashof number increases from 1300 to 4000, displayed in Figure 8. Furthermore, by increasing Grashof number to more than 4000, the results indicate that the wake flow vanishes and disappear, and the flow becomes entirely attached to the cylinder surface without any separation. Therefore, it can be obviously concluded that the thermal buoyancy forces can significantly affect the flow behavior behind the cylinder; thus, they can control or eliminate forming the vortex shedding, as well as reduce or eliminate forming the wake flow. Indeed, this phenomenon may decrease the drag forces on the cylinder exposed to the vertical flow stream.

Moreover, the figures also show how the changing in the flow behavior the rear of the cylinder affect the shape of the thermal plume in this region, also the thickness of the thermal boundary layer formed on the cylinder wall. Therefore, this can change the heat transfer from the cylinder as it will be seen later.

Another important objective of the current study is to investigate energy exchange from the cylinder to the adjacent flowing fluid. For this purpose, the variations of transient mean Nusselt number are shown in Figure 10 for Grashof numbers of 0 and 1300 when the vortex shedding exists, and in Figure 11 for Grashof number more than 1400, when the flow becomes completely steady flow. In Figure 10, one can see that at Gr = 0 and 1300, the behavior of the mean Nusselt number with the time after a long transient period becomes fully periodic. Also, this transient period increases significantly as Grashof number increase from 0 to 1300. In addition, importantly the increase in Grashof number leads to a slight increase in the mean Nusselt number. However, in Figure 11, the results show that the behavior of the mean Nusselt number with the time after a short transient period becomes fully steady for Gr ≥ 1400. Also, the transient period is shown to be decreased as Grashof number increases. Surprisingly, the results reveal that for the increase in Grashof number from 1400 to 4000, the amount of mean Nusselt number decreases slightly as Grashof number increases. This is when the twin vortices (wake flow) behind the cylinder exist. But, for the increase in Grashof

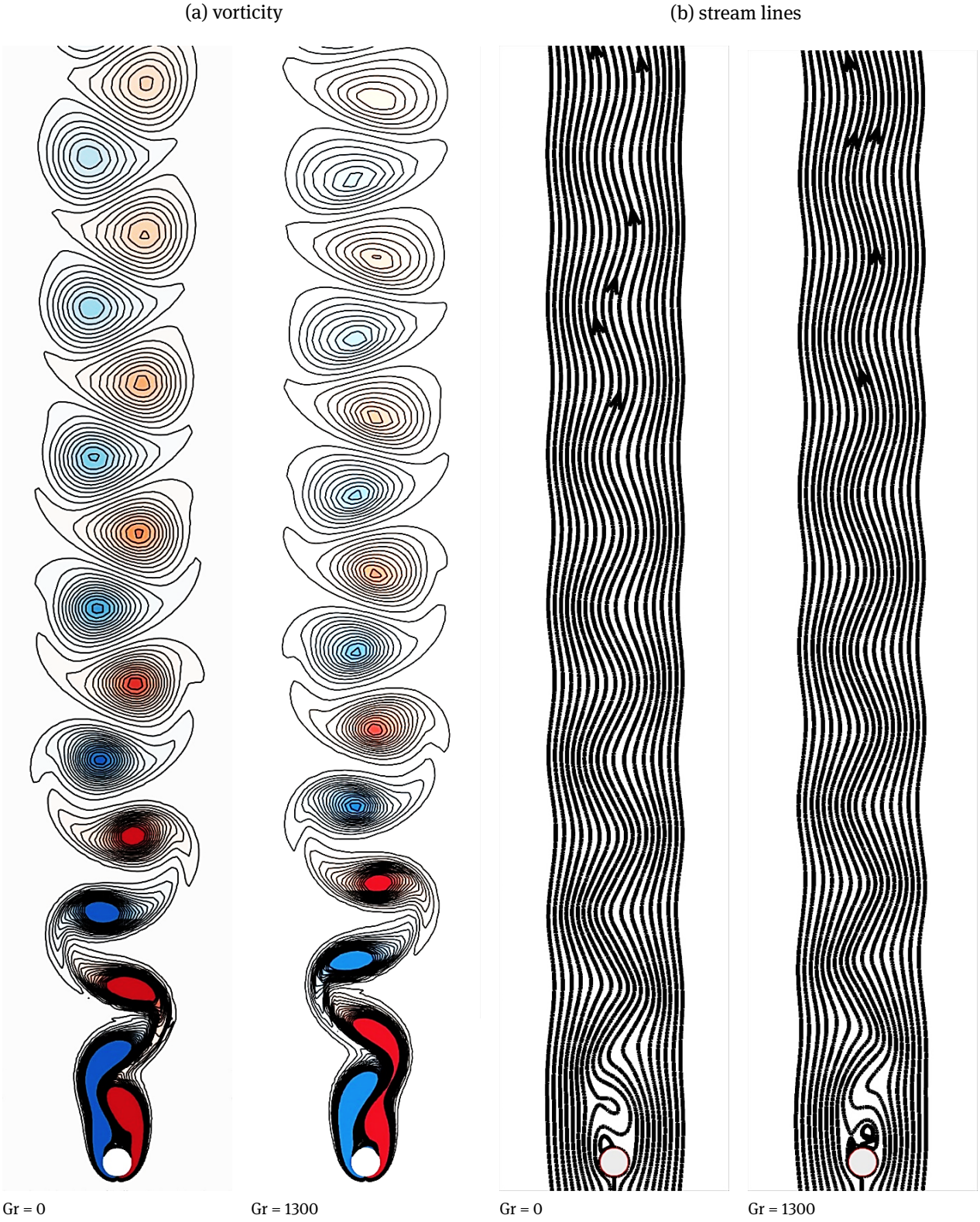

Figure 4: (a) Vorticity patterns, and (b) streamlines, for two Grashof numbers Gr = 0.0 and 1300, at Re = 100

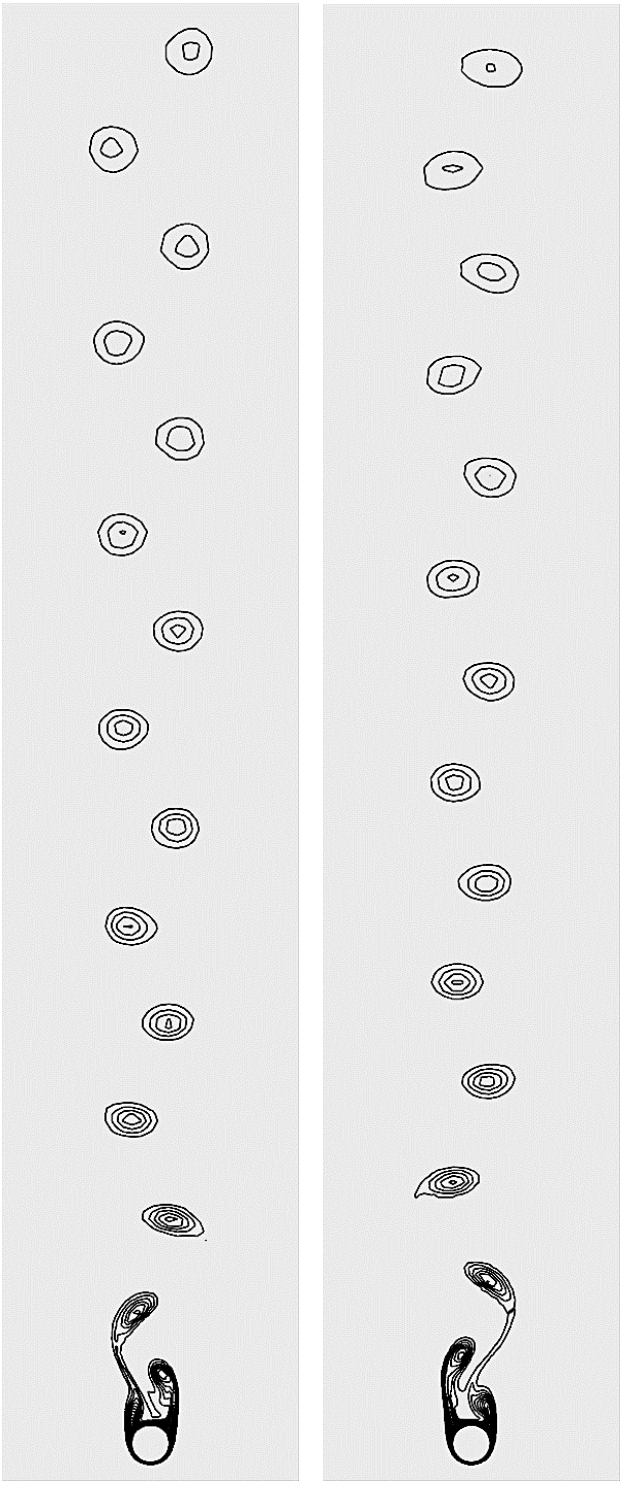

Gr = 0 Gr = 1300

Figure 5: Isotherms patterns for two Grashof numbers Gr = 0.0 and 1300, at Re = 100

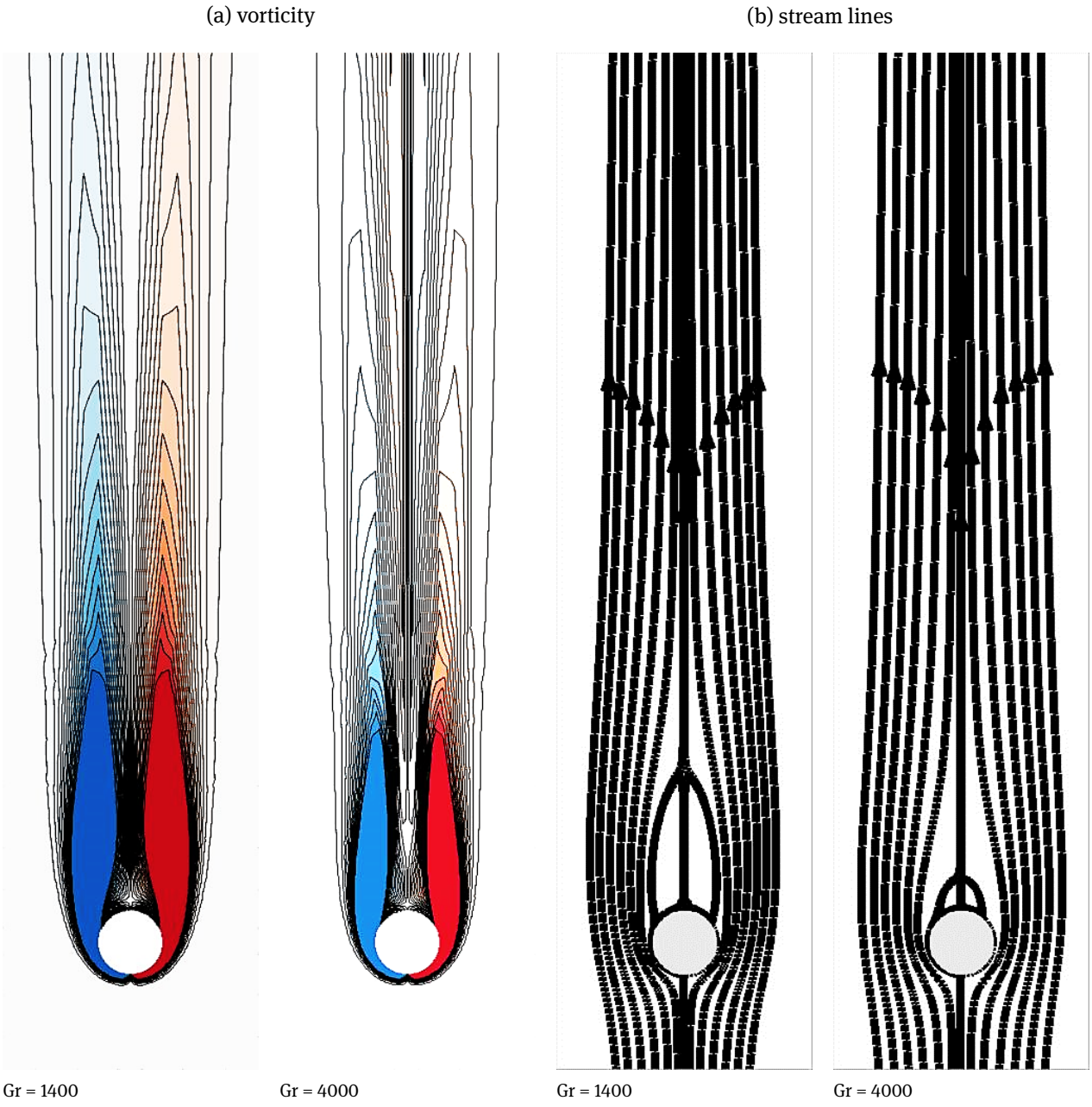

Figure 6: (a) Vorticity patterns, and (b) streamlines, for two Grashof numbers Gr = 1400 and 4000, at Re = 100

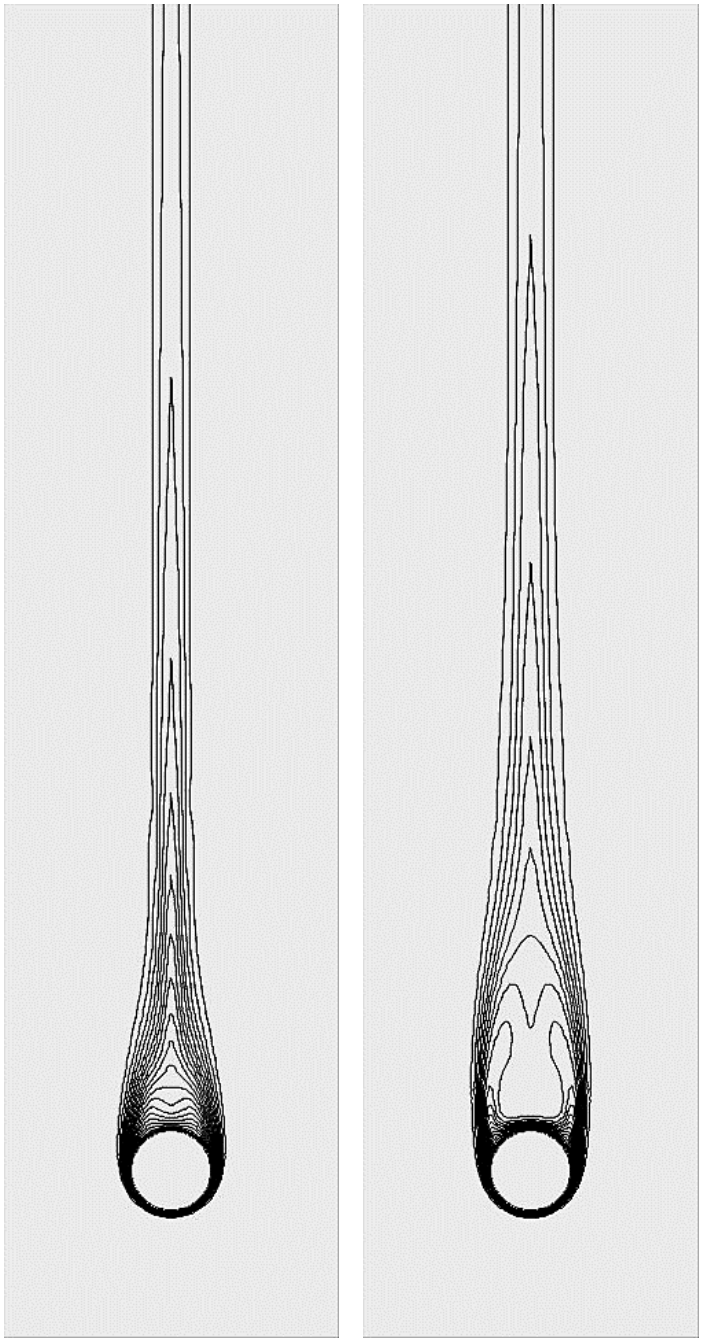

Gr = 1400 Gr = 4000

Figure 7: Isotherms patterns for two Grashof numbers Gr = 1400 and 4000, at Re = 100

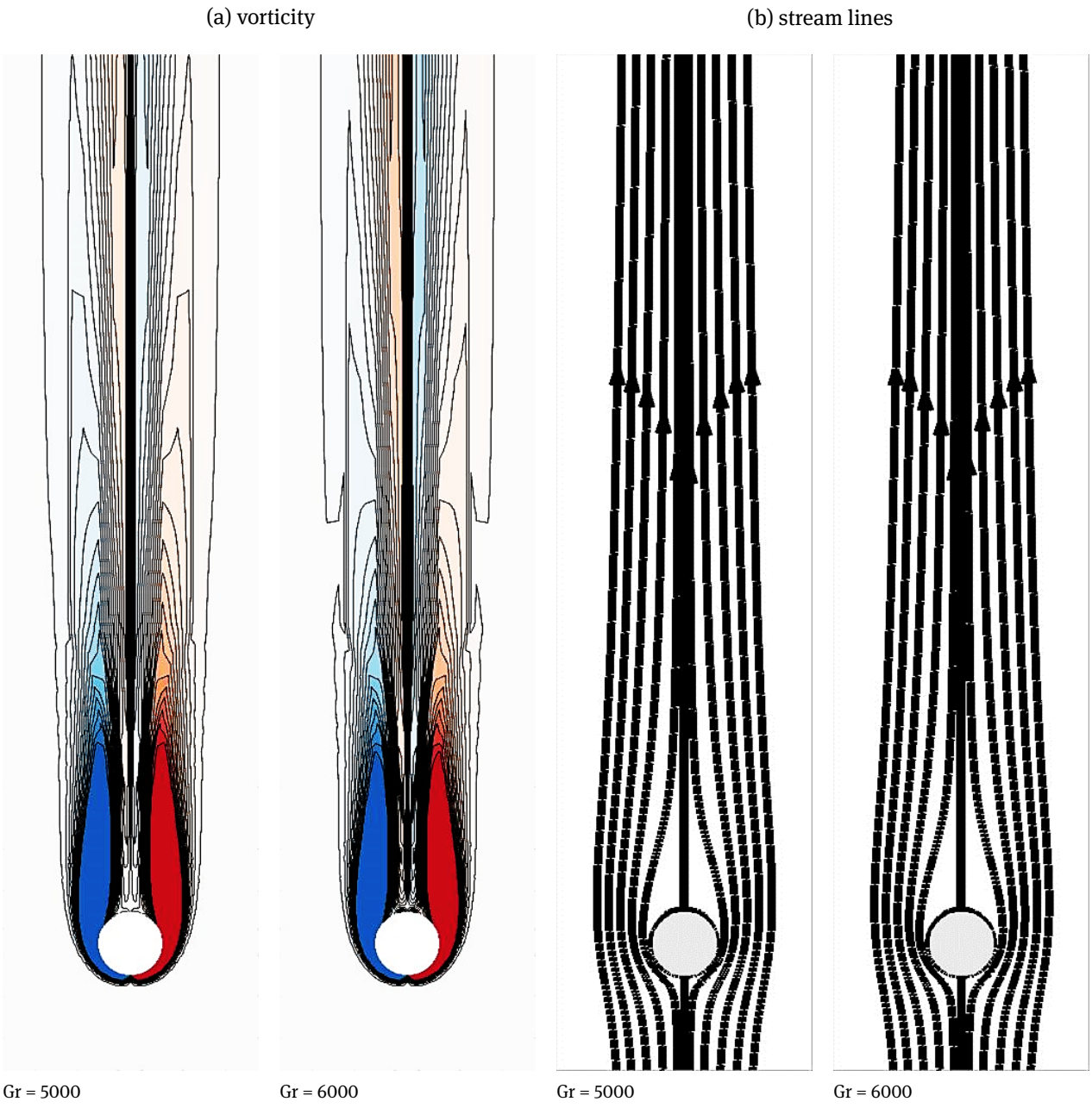

Figure 8: (a) Vorticity patterns, and (b) streamlines, for two Grashof numbers Gr = 5000 and 6000, at Re = 100

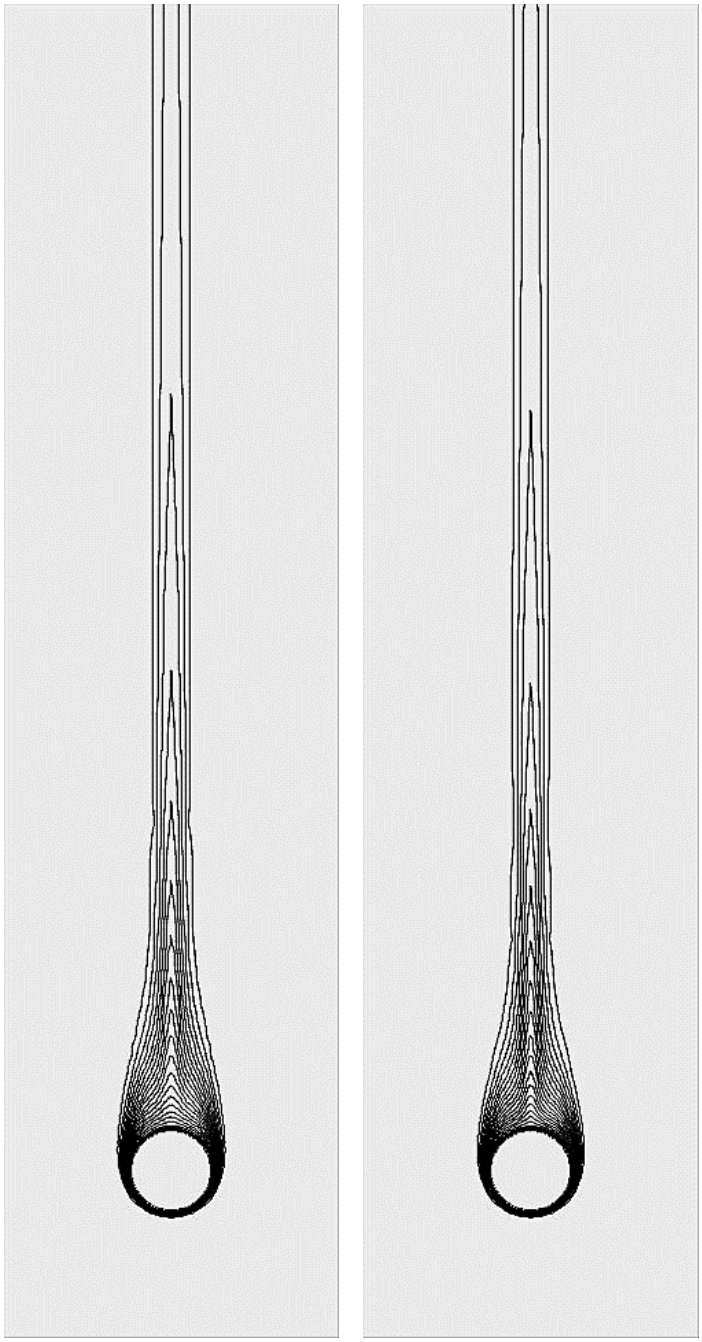

Gr = 5000 Gr = 6000

Figure 9: Isotherms patterns for two Grashof numbers Gr = 5000 and 6000, at Re = 100

number from 5000 to 6000, when these twin vortices disappear and the flow becomes completely attached along the cylinder surface, the effect of Grashof number on mean Nusselt number alters. Thus, it is seen that the mean Nusselt number starts increasing as Grashof number increases.

For best understanding to the flow characteristics under the instability situation, a series of images for the instantaneous streamlines, vorticity, and isotherms patterns, are shown in Figures 12-15 over full periodic cycles of oscillation in Nusselt number, which, which corresponds to full vortex shedding period at Gr = 0 and 1300, respectively. It is seen that in this instability, a couple of eddies is developed, and is shed alternately in the downstream direction. The figures show that for both cases of Grashof numbers, similar mode of periodicity is produced, with a slight increase in the oscillation amplitude and frequency is observed at Gr = 1300. The images of the vorticity depict the formation and shedding of the positive (blue) and negative (red) vortices in the wake region during the shedding period. The images also depict the development of the thermal wake associated with the hydro-dynamic wake at the same cycle times. It is shown that the thermal boundary layer after the cylinder splits and transfers within the wake zone, and the hot plumes emerging in the places of the wake eddies. In fact, as the wake eddies are rolling up and shedding periodically behind the cylinder, as the thermal boundary layer on the cylinder wall changes producing a clear fluctuation in Nusselt number with the time, as demonstrated in the upper plots of each figure.

The distribution of local Nusselt number Nu_L along the cylinder circumference for a polar angle between θ° = 0–360° is illustrated in Figure 16 for different Grashof numbers Gr = 0–5000, at Re = 100. The positions of θ° = 90° and 270° represent the rear and the front stagnation points in relation to the incoming flow air. It can be seen that as Grashof number increases, the local Nusselt number increases minimally over the surface close to the front separation point owing to the huge fluid acceleration, which reduces significantly the thickness of the boundary layer in this area of the cylinder. At low Grashof number Gr ≤ 1400, the minimum local Nusselt number occurs at the sides of the cylinders of $\theta^\circ \approx 40^\circ$ and $\approx 140^\circ$. However, as Grashof increases behind Gr ≥ 4000, the local Nusselt number decrease in the back area between , until the minimum local Nusselt number occurs at the rare separation point of the cylinder at $\theta^\circ \approx 90^\circ$. This is attributable to the heating effect, which suppresses the vortex shedding, delays the flow separation, and shifts the points of separation from the cylinder sides into the rare point until the complete flow attachment is happened around the cylinder, and the flow separation is vanished.

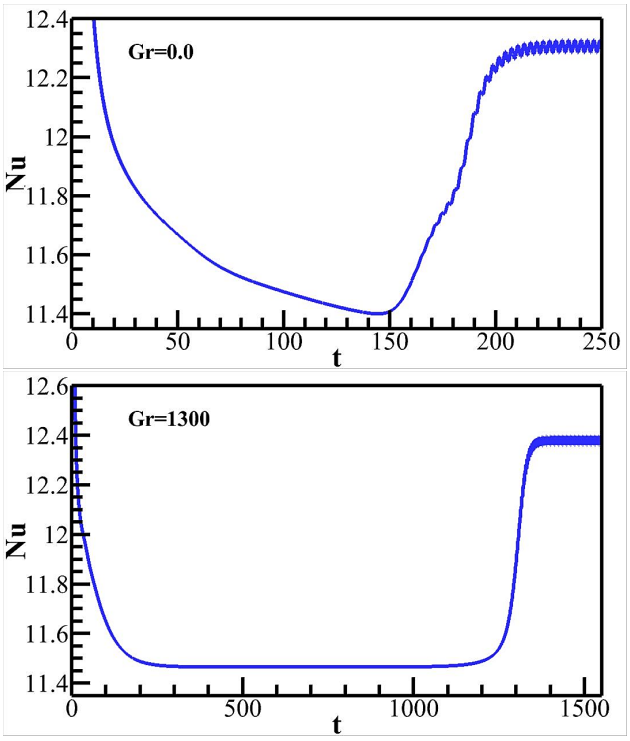

Figure 10: Transient behavior of Nusselt number with the time, Grashof numbers Gr = 0.0 and 1300, at Re = 100

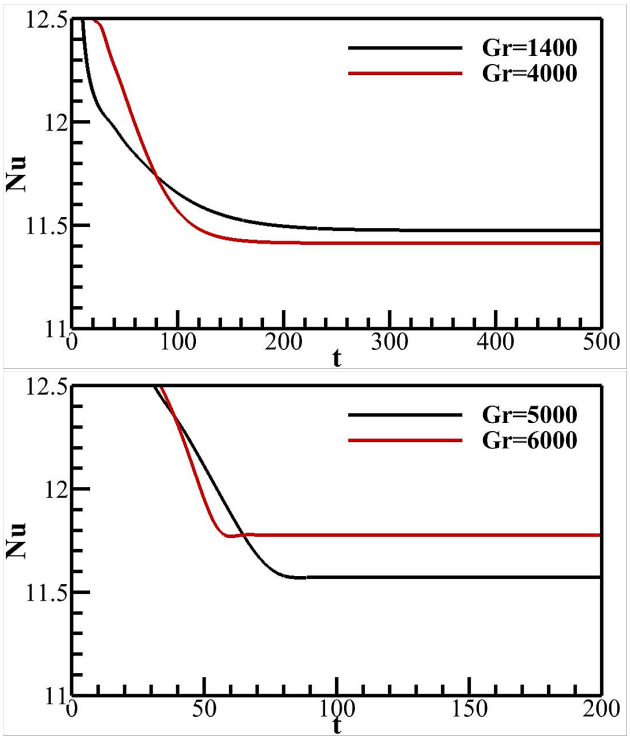

Figure 11: Transient behavior of Nusselt number with the time, Grashof numbers Gr = 1400, 4000, 5000 and 6000, at Re = 100

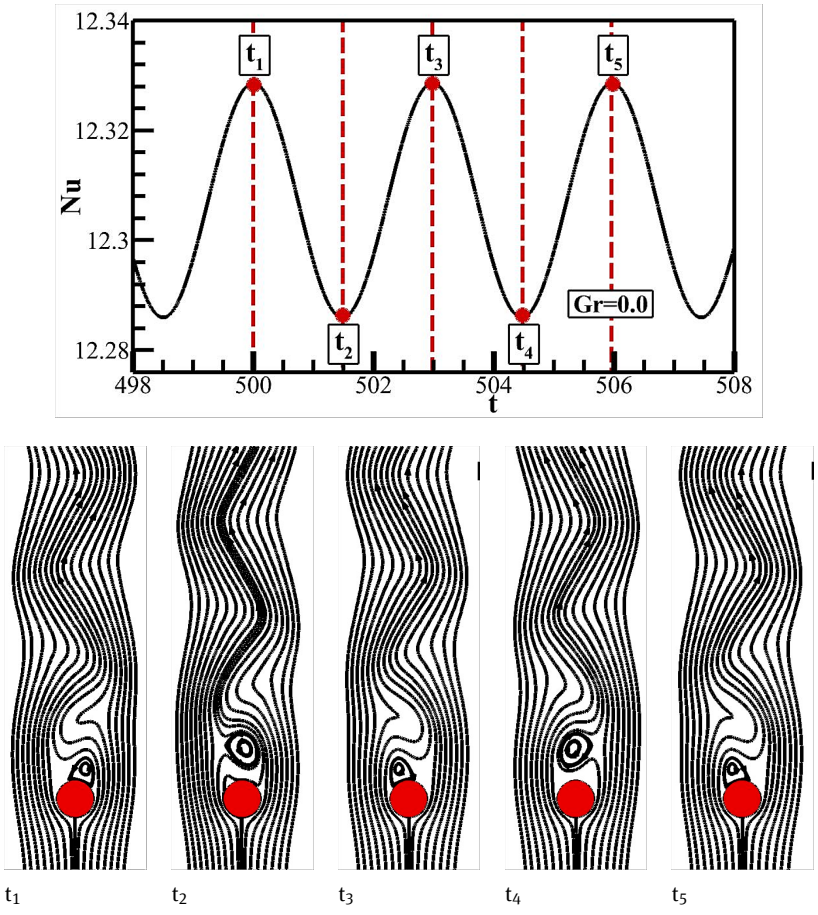

Figure 12: Stream patterns over a half-full transient period at Grashof number Gr = 0.0 and Re = 100

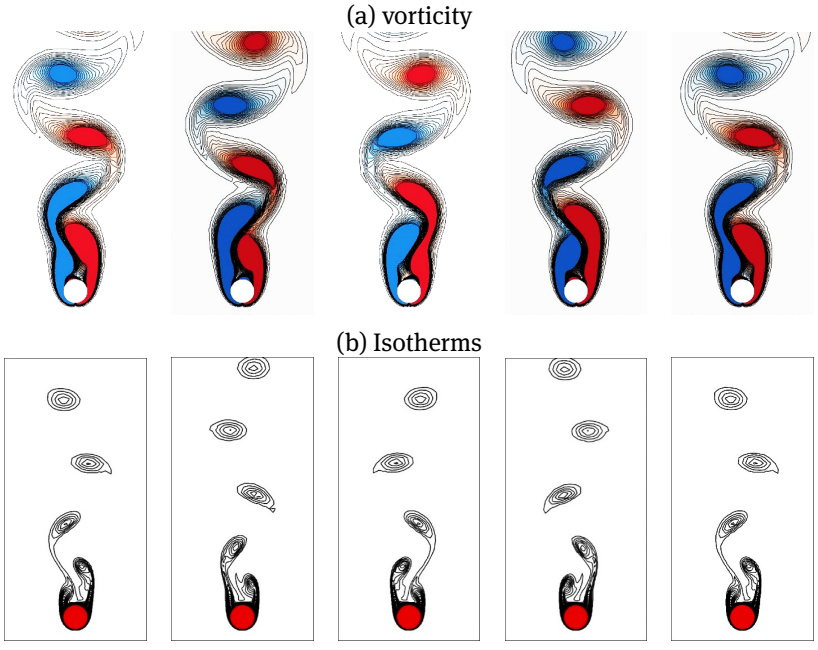

Figure 13: (a) Vorticity, and (b) isotherms, patterns over a half-full transient period at Grashof number Gr = 0.0 and Re = 100

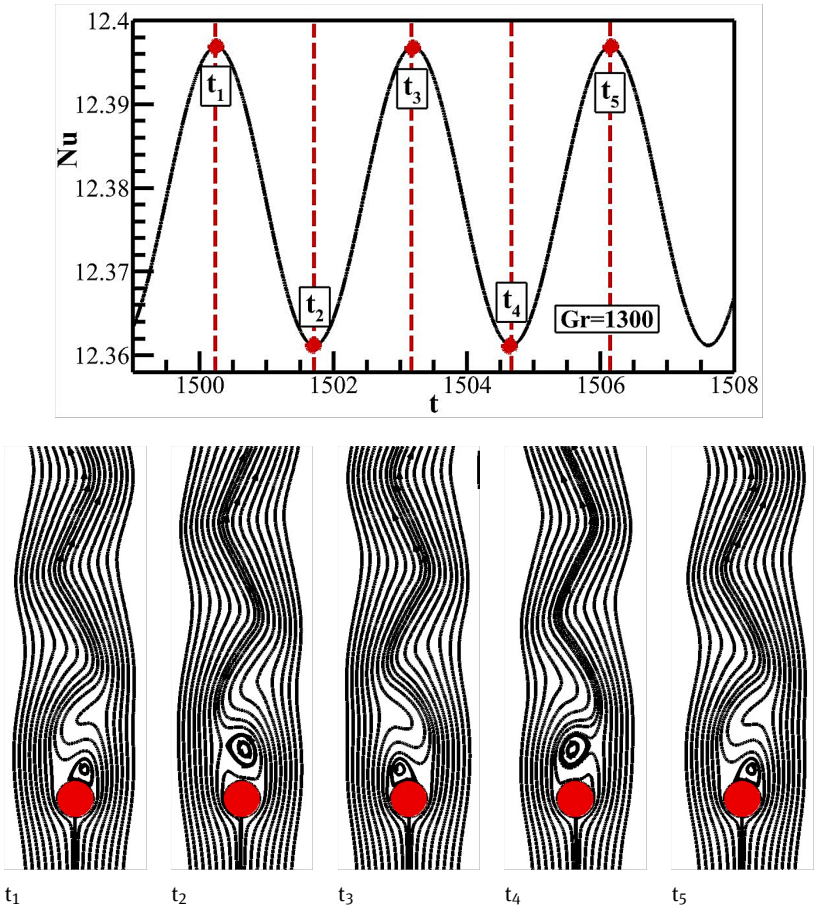

Figure 14: Stream patterns over a half-full transient period at Grashof number Gr = 1300 and Re = 100

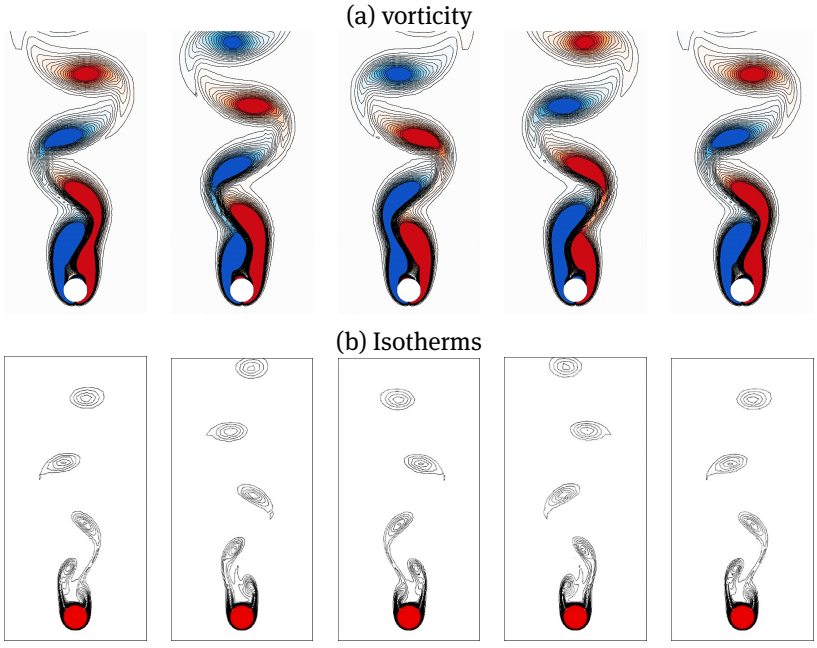

Figure 15: (a) Vorticity, and (b) isotherms, patterns over a half-full transient period at Grashof number Gr = 1300 and Re = 100

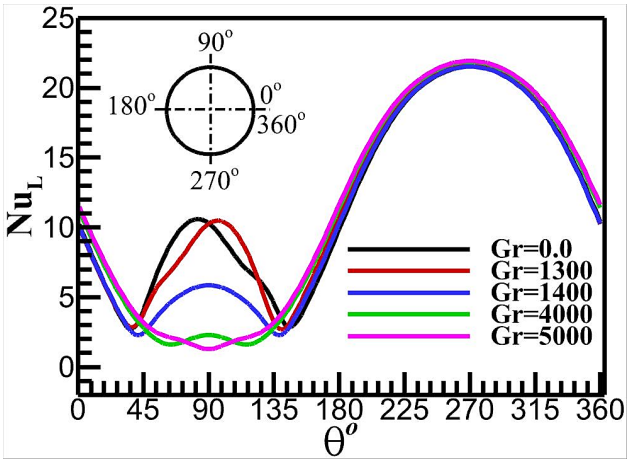

Figure 16: Distribution of local Nusselt number around the cylinder at different Grashof numbers and Re = 100

5 Conclusions

In this study, fluid flow and heat transfer characteristics around a circular cylinder under the effect of mixed convection, and positioned in an incompressible and laminar vertical air stream are investigated numerically employing the finite volume method. The elimination of vortex shedding formed behind the cylinder, which can increase in the drag forces, by the heating effect was studied for different Grashof numbers $0 \leq Gr \leq 6000$, and at Reynolds number Re = 100. The results showed that for low and moderate Grashof numbers $Gr \leq 1300$, a Van Karman vortex street is generated back into the cylinder. Also, as Grashof number increases for the range of $1400 \leq Gr \leq 4000$, this vortex shedding vanishes and converts into steady couple of eddies attached to the cylinder back. Moreover, further increase in Grashof number for Gr ≥ 5000, these twin eddies shrink considerably disappear, and the flow becomes entirely attached to the cylinder surface without any separation. The mean Nusselt number is found to increases slightly as Grashof number increases from 0 to 1300, for the unsteady flow situation. However, surprisingly, the mean Nusselt number is shown to decrease as Grashof number increases in the steady flow region with the existence of twin vortices behind the cylinder. Nevertheless, for further increase in Grashof number behind Gr ≥ 5000, the mean Nusselt number alters to increase as Grashof number increases. It is found that the local Nusselt number is not affected considerably by heating effect in the area close to the front separation point. However, the considerable alteration in local Nusselt number occurs in the rare area of the cylinder between $\theta^\circ \approx 40^\circ$ and $\approx 140^\circ$.

Funding information: The authors state no funding involved.

Author contributions: All authors have accepted responsibility for the entire content of this manuscript and approved its submission.

Conflict of interest: The authors state no conflict of interest.

References

[1] Li Z, Navon IM, Hussaini MY, Le Dimet FX. Optimal control of cylinder wakes via suction and blowing. Comput Fluids. 2003;32(2):149–71.
[2] Mittal S. Control of flow past bluff bodies using rotating control cylinders. J Fluids Struct. 2001;15(2):291–326.
[3] Muddada S, Patnaik BS. An active flow control strategy for the suppression of vortex structures behind a circular cylinder. Eur J Mech B Fluids. 2010;29(2):93–104.
[4] Shukla RK, Arakeri JH. Minimum power consumption for drag reduction on a circular cylinder by tangential surface motion. J Fluid Mech. 2013;715:597–641.
[5] Subhash Reddy M, Muddada S, Patnaik BS. Flow past a circular cylinder with momentum injection: optimal control cylinder design. Fluid Dyn Res. 2013;45(1):015501.
[6] Badr HM. Laminar combined convection from a horizontal cylinder-Parallel and contra flow regimes. Int J Heat Mass Transf. 1984;27(1):15–27.
[7] Chang K-S, Sa J-Y. The effect of buoyancy on vortex shedding in the near wake of a circular cylinder. J Fluid Mech. 1990;220:253-266.
[8] Wang CY. Mixed convection on a vertical needle with heated tip. Phys Fluids A Fluid Dyn. 1990;2(4):622–5.
[9] Michaux-Leblond N, B'elorgey M. Near-wake behavior of a heated circular cylinder: viscosity-buoyancy duality. Exp Therm Fluid Sci. 1997;15(2):91–100.
[10] Varaprasad Patnaik BS, Aswatha Narayana PA, Seetharamu KN. Numerical simulation of vortex shedding past a circular cylinder under the influence of buoyancy. Int J Heat Mass Transf. 1999;42(18):3495–507.
[11] Kieft RN, Rindt CC, Van Steenhoven AA, van Heijst GJ. On the wake structure behind a heated horizontal cylinder in cross-flow. J Fluid Mech. 2003;486:189–211.
[12] Biswas G, Sarkar S. Effect of thermal buoyancy on vortex shedding past a circular cylinder in cross-flow at low Reynolds numbers. Int J Heat Mass Transf. 2009;52(7-8):1897–912.
[13] Sharma N, Dhiman AK, Kumar S. Mixed convection flow and heat transfer across a square cylinder under the influence of aiding buoyancy at low Reynolds numbers. Int J Heat Mass Transf. 2012;55(9-10):2601–14.
[14] Gandikota G, Amiroudine S, Chatterjee D, Biswas G. The effect of aiding/opposing buoyancy on two-dimensional laminar flow across a circular cylinder, Numeric. Numer Heat Transf A. 2010;58(5):385–402.

[15] Guillén I, Treviño C, Martinez-Suástegui L. Unsteady laminar mixed convection heat transfer from a horizontal isothermal cylinder in contraflow: buoyancy and wall proximity effects on the flow response and wake structure. Exp Therm Fluid Sci. 2014;52:30–46.
[16] Sanyal A, Dhiman A. Wake interactions in a fluid flow past a pair of side-by-side square cylinders in presence of mixed convection. Phys Fluids. 2017;29(10):103602.
[17] Chatterjee D. Triggering vortex shedding by superimposed thermal buoyancy around bluff obstacles in cross-flow at low Reynolds numbers. Numer Heat Tr Appl. 2012;61(10):800–6.
[18] Chatterjee D. Dual role of thermal buoyancy in controlling layer separation around bluff obstacles. Int Commun Heat Mass Transf. 2014;56:152-8.
[19] Chatterjee D, Mondal B. Effect of thermal buoyancy on vortex shedding behind a square cylinder in cross flow at low Reynolds numbers. Int J Heat Mass Transf. 2011;54(25-26):5262-74
[20] Chatterjee D, Mondal B. Effect of thermal buoyancy on the two-dimensional upward flow andheat transfer around a square cylinder. Heat Transf Eng. 2012;33(12):1063–74.
[21] Chatterjee D, Mondal B. On the vortex shedding mechanism behind a circular cylinder subjected to cross buoyancy at low Reynolds numbers. Comput Therm Sci. 2012;4(1):23–38.
[22] Chatterjee D, Mondal B. Control of flow separation around bluff obstacles by superimposed thermal buoyancy. Int J Heat Mass Transf. 2014;72:128–38.
[23] Van Doormal JP, Raithby GD. Enhancement of the simple methods for predicting incompressible fluid flows. Numer Heat Transf A. 1984;7:147–63.
[24] Nasr K, Ramadhyani S, Viskanta R. Experimental investigation a forced convection heat transfer from a cylinder embedded in a packed bed. J Heat Transf. 1994;116(1):73–80.